Supporting Information

All-Textile Triboelectric Sensor for Wearable Teleoperated Human-Machine Interaction

Qiang He[a], Yufen Wu[b], Zhiping Feng[a], Wenjing Fan[a], Zhiwei Lin[a], Chenchen Sun[a], Zhihao Zhou[a], Keyu Meng[a], Wenzhuo Wu[*c] and Jin Yang[*a]

[a] Key Laboratory of Optoelectronic Technology & Systems (Ministry of Education), Department of Optoelectronic Engineering, Chongqing University, Chongqing 400044, China.

[b] College of Physics and Electronic Engineering Chongqing Normal University, Chongqing 401331, China.

[c] School of Industrial Engineering, Purdue University, West Lafayette, Indiana 47907, USA.

Corresponding authors at:
School of Industrial Engineering, Purdue University, West Lafayette, Indiana 47907, USA.
Department of Optoelectronic Engineering, Chongqing University, Chongqing 400044, China.
Address correspondence to: wenzhuowu@purdue.edu, yangjin@cqu.edu.cn

Table S1. Performances compare of textile pressure sensors

Working mechanism	Sensitivity	Detection limit	Range	References
resistance	14.4 kPa^{-1}	2 Pa	2~2800 Pa	1
resistance	0.358 mA kPa^{-1}	-	<60 kPa	2
resistance	1.03 kPa^{-1}	20 mg	<10 kPa	3
capacitance	0.21 kPa^{-1}	-	<3.9 MPa	4
resistance	0.012 kPa^{-1}	1.27 kPa	1.27<254 kPa	5
piezoelectric	1.1 V kPa^{-1}	0.1 Pa	-	6
resistance	18.376 kPa^{-1}	2 Pa	0.002~10 kPa	7
triboelectric	6.23 mV kPa^{-1}	362 Pa	0.362 ~ 326 kPa	8
triboelectric	-	0.98 N	0.98 ~147 N	9
triboelectric	0.77V Pa^{-1}	-	<14 kPa	10
triboelectric	0.385V kPa^{-1}	2.6 kPa	2.6~400 kPa	11
triboelectric	1.1 V kPa^{-1}	100 Pa	0.1~400 kPa	This work

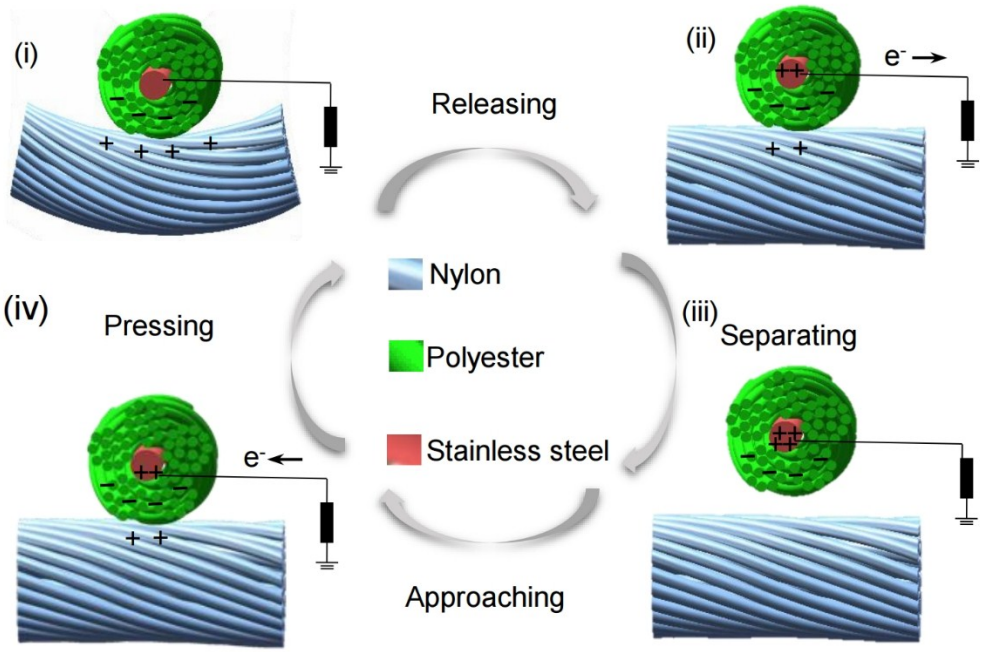

Figure S1. The working mechanism of the ATTS

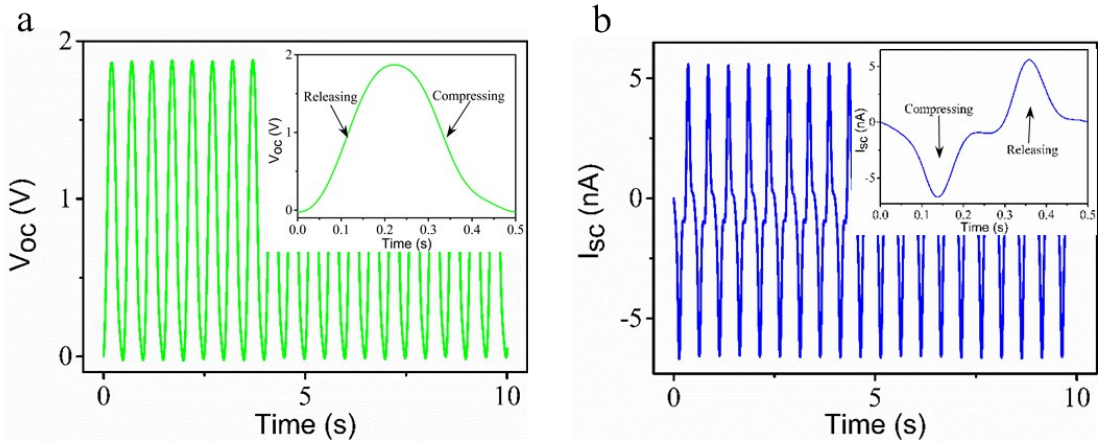

Figure S2. The open-circuit voltage (a) and the short-circuit current (b) under applied forces of 20 N at 2 Hz

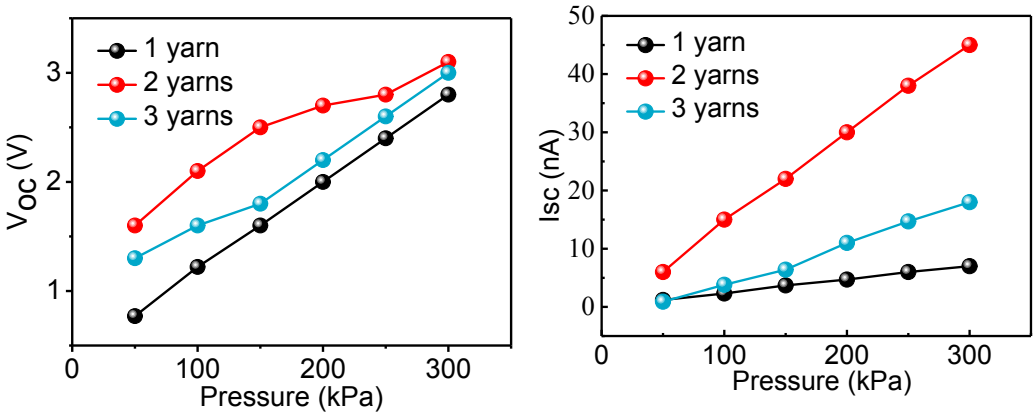

Figure S3. The open-circuit voltages (a) the short-circuit current (b) in the pressure region from 50 kPa to 300 kPa for three ATTSs sewn with different numbers of sensing yarns

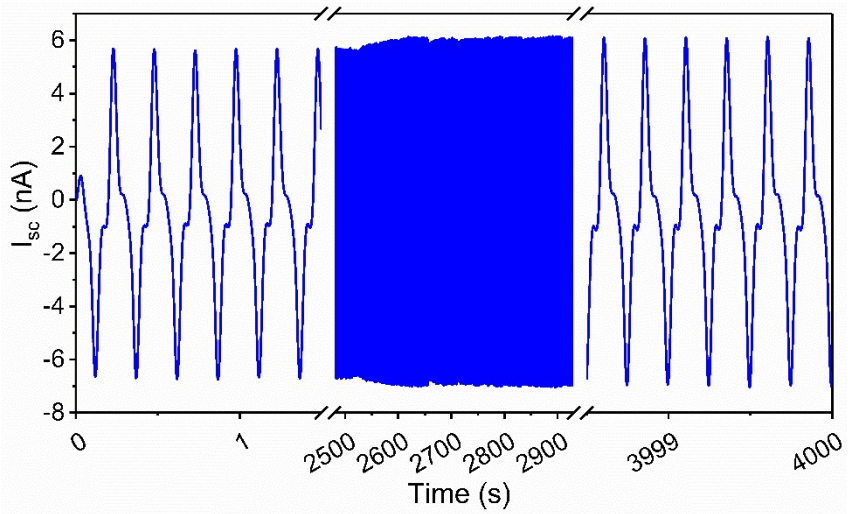

Figure S4. The mechanical durability characterization of the ATTS under an applied force (20 N, 4 Hz) for 16000 cycles.

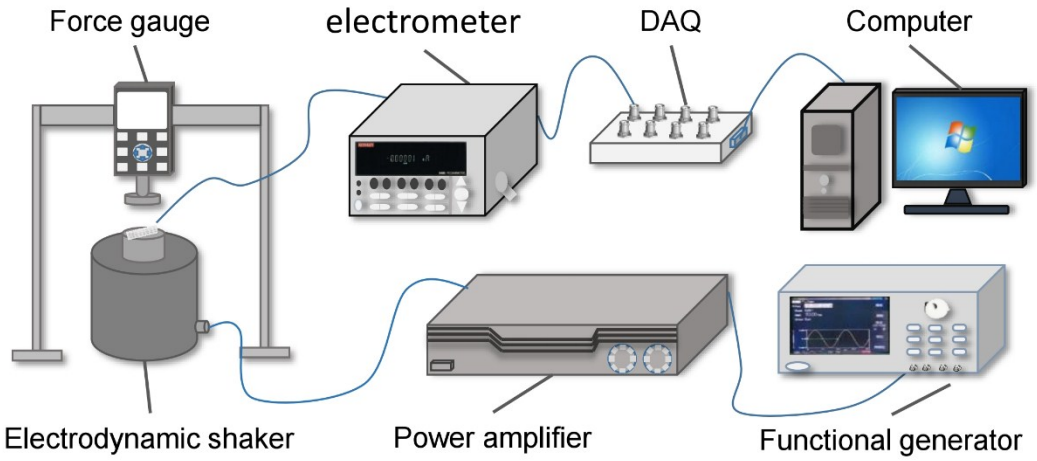

Figure S5. Experimental setup to analyze the electrical output performance of the ATTS

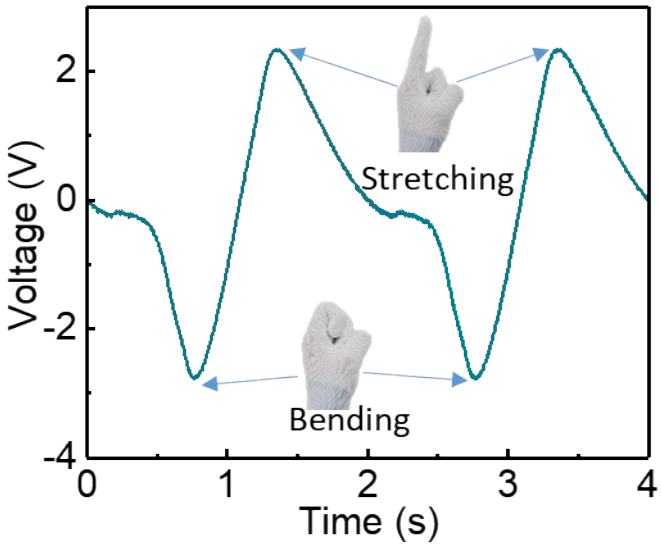

Figure S6. The output voltage of the ATTS-integrated glove during two cycles of the finger bending and stretching process. Negative voltages obtained in bending cycles while positive voltages obtained in stretching cycles, demonstrating the polarity of the output voltage in the bending and stretching process.

Reference

1 M. Liu, X. Pu, C. Jiang, T. Liu, X. Huang, L. Chen, C. Du, J. Sun, W. Hu and Z. L. Wang, *Adv. Mater.*, 2017, **29**, 1703700.

2 N. Luo, J. Zhang, X. Ding, Z. Zhou, Q. Zhang, Y. T. Zhang, S. C. Chen, J. L. Hu and N. Zhao, Adv. Mater. Technol., 2017, 3, 1700222.

3 S. Chen, S. Liu, P. Wang, H. Liu and L. Liu, J. Mater. Sci., 2018, 53, 2995-3005.

4 J. Lee, H. Kwon, J. Seo, S. Shin, J. H. Koo, C. Pang, S. Son, J. H. Kim, Y. H. Jang, D. E. Kim and T. Lee, *Adv. Mater.*, 2015, **27**, 2433-2439.

5 S. J. Kim, W. Song, Y. Yi, B. K. Min, S. Mondal, K. S. An and C. G. Choi, *ACS Appl. Mater. Interface*s, 2018, **10**, 3921-3928.
6 L. Persano, C. Dagdeviren, Y. Su, Y. Zhang, S. Girardo, D. Pisignano, Y. Huang and J. A. Rogers, *Nat. Commun.*, 2013, **4**, 1633.
7 Y. Zhou, J. He, H. Wang, K. Qi, N. Nan, X. You, W. Shao, L. Wang, B. Ding and S. Cui, *Sci. Rep.*, 2017, **7**, 12949.
8 Y.-E. Shin, J.-E. Lee, Y. Park, S.-H. Hwang, H. G. Chae and H. Ko, *J. Mater. Chem. A*, 2018, **6**, 22879–22888.
9 W. Seung, M.K. Gupta, K.Y. Lee, K.S. Shin, J.H. Lee, T.Y. Kim, S. Kim, J. Lin, J.H. Kim, S.W. Kim, *ACS Nano*, 2015, **9**, 3501-3509.
10 Z. Lin, J. Yang, X. Li, Y. Wu, W. Wei, J. Liu, J. Chen and J. Yang, *Adv. Funct. Mater.*,2018, **28**, 1704112.
11 R. Cao, J. Wang, S. Zhao, W. Yang, Z. Yuan, Y. Yin, X. Du, N. W. Li, X. Zhang, X. Li, Z. L. Wang and C. Li, *Nano Res.*, 2018, **11**, 3771-3779.